# Influence of oceanic heat variability on sea ice anomalies in the Nordic Seas

P. Schlichtholz[1]

Received 19 October 2010; revised 2 February 2011; accepted 7 February 2011; published 9 March 2011.

[1] A strong control of sea ice area (SIA) in the Nordic Seas in the period 1982–2006 by oceanic heat variability is reported. In particular, variability of summer Atlantic water temperature in the Barents Sea Opening explains about 75% of the variance of the following winter SIA anomalies which opens prospects for seasonal predictability of regional sea ice cover. A strong link of winter SIA anomalies to variability in the previous spring sea surface temperature on the western (Greenland Sea) and eastern (Barents Sea) sides of the Nordic Seas indicates that the oceanic control of sea ice cover in these areas mainly results from postsummer surface reemergence of oceanic heat anomalies generated by earlier atmospheric forcing. In particular, late winter North Atlantic Oscillation and anomalous winds across the Barents Sea ice edge significantly influence next winter sea ice cover on the western and eastern sides of the Nordic Seas, respectively.
**Citation:** Schlichtholz, P. (2011), Influence of oceanic heat variability on sea ice anomalies in the Nordic Seas, *Geophys. Res. Lett.*, *38*, L05705, doi:10.1029/2010GL045894.

## 1. Introduction

[2] Arctic sea ice is a key component of the climate system. Its extent is subject to strong natural variability on different timescales [e.g., *Vengas and Mysak*, 2000] and very sensitive to global warming triggered by anthropogenic increases in atmospheric greenhouse gases [e.g., *Serreze et al.*, 2007]. As in the future these increases should accelerate the recently observed decline in summertime Arctic sea ice cover [e.g., *Holland et al.*, 2006], seasonal forecasting of sea ice is becoming of greater interest for operational shipping, natural resources, fisheries, and native populations, as well as for input into seasonal weather forecasting models. In response to this interest several institutions develop sea ice forcast techniques based on statistical relationships between observed variables or ice-ocean coupled models with prescribed atmospheric forcing [e.g., *Drobot et al.*, 2008; *Zhang et al.*, 2008]. Ice-ocean and climate coupled models indicate that both summer and winter Arctic sea ice conditions exhibit some predictability [e.g., *Lindsay et al.*, 2008; *Holland et al.*, 2010].

[3] Forecasting of winter sea ice is of great importance in the regional context of the Nordic (Greenland-Iceland-Norwegian and Barents) Seas (Figure 1) where winter sea ice extent anomalies may trigger a dynamic atmospheric response [e.g., *Wu et al.*, 2004], with severe consequences for whether conditions over northern continents [*Petoukhov and Semenov*, 2010]. Sea ice responds to changing conditions in both the atmosphere and ocean. Relatively long ocean advective timescales imply that sea ice cover in the Nordic Seas could potentially be predicted from upstream anomalies of Atlantic water temperature (AWT) transported northward by the Norwegian Atlantic Current (NwAC in Figure 1) if sea ice response to these anomalies was strong. Links between sea ice extent variability in the Barents Sea and upstream AWT anomalies observed, e.g., 2–3 years earlier in the southern Norwegian Sea indeed exist [e.g., *Vinje*, 2001]. However, the AWT anomalies are strongly modified all along their pathway through the Nordic Seas (Figure 1, arrows) by local variability in air-sea interactions during cold seasons [*Schlichtholz and Houssais*, 2011]. Therefore, oceanic heat anomalies observed downstream of the Norwegian Atlantic Current could be a better predictor of regional sea ice variability.

[4] Here we show that recent variations of wintertime sea ice cover in the Nordic Seas are indeed tightly linked to earlier anomalies of AWT in the Barents Sea Opening (BSO) area (Figure 1, box) and sea surface temperature (SST) in the Barents and Greenland seas. Relation of these links to the most prominent mode of recurrent large-scale atmospheric variability in the extratropical northern hemisphere, i.e., the North Atlantic Oscillation (NAO) [e.g., *Hurrell et al.*, 2003] is analyzed. As influences of the NAO on the Nordic Seas ice cover are time dependent [e.g., *Vinje*, 2001] and recent interannual variability of wintertime sea ice extent in the Barents Sea was considerably influenced by simultaneous local wind anomalies [*Sorteberg and Kvingedal*, 2006], we also consider relation to anomalous winds over the Barents Sea.

## 2. Data and Methods

[5] Seasonal mean fields of SST (see Table 1 for acronyms) and sea ice concentration (SIC) in the Nordic Seas are constructed from *Reynolds et al.*'s [2002] monthly mean fields, which are averaged over 4 months with the interval of 1 month. The 4-month seasonal averaging is carried out for consistency with the study by *Schlichtholz and Houssais* [2011] where an index (detrended and normalized anomalies) of summer AWT variability in the Atlantic water core (100–300 m) in the BSO box (13–17°E, 70–76°N, Figure 1) was constructed using June–September temperature profiles from the Oceanographic Database of the International Council for the Exploration of the Sea (http://www.ices.dk/) and the World Ocean Database of the US National Oceanographic Data Center (http://www.nodc.noaa.gov/). The index covers the period 1982–2005 (Figure 2, circles) for

[1]Institute of Oceanology, Polish Academy of Sciences, Sopot, Poland.


0094-8276/11/2010GL045894

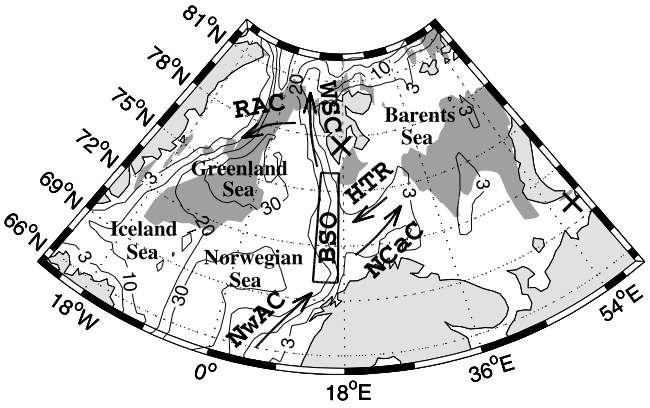


**Figure 1.** Bathymetry (in $10^2$ m) in the Nordic Seas area. The arrows depict major pathways of Atlantic water: the Norwegian Atlantic Current (NwAC), North Cape Current (NCaC), West Spitsbergen Current (WSC), Return Atlantic Current (RAC), and Hopen Trench Recirculation (HTR). The crosses indicate the points for calculation of the OIW index (see Table 1 for definition). Dark shading denotes the area of significant early winter (November–February) SIC anomalies regressed onto the previous summer (June–September) index of AWT variability in the BSO box in the 1982–2005 period (Figure 2, circles).

which statistically meaningful estimates of summer AWT in the BSO box could be obtained. As the same index is used here, the study is limited to the period 1982–2006.

[6] For each season, fields of interannual SIC and SST anomalies are obtained by removing from the local time series their linear trends. A seasonal index of total sea ice area (SIA) variability in the Nordic Seas is obtained by dividing the SIC anomalies integrated over the full domain of Figure 1 by their standard deviation. Analogous indices of SIA variability in the marginal ice zone (MIZ) of the eastern and western parts of the Nordic Seas are based on

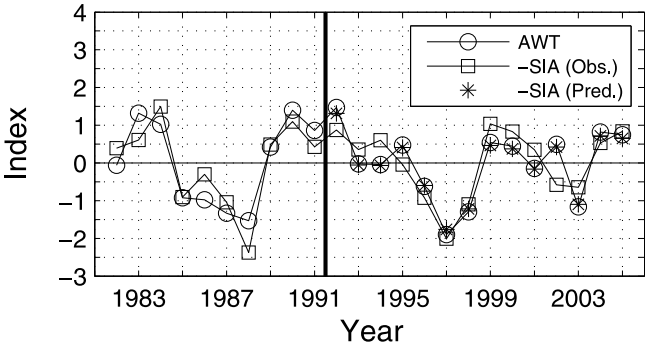


**Figure 2.** Detrended and normalized anomalies of AWT in the BSO area (box in Figure 1) in the 1982–2005 period (circles) and the following early winter total SIA in the Nordic Seas (squares). The sign of the SIA anomalies is reversed. The stars to the right of the bold vertical line show a prediction of the SIA anomalies from the AWT anomalies in the 1992–2005 subperiod based on a linear model of the relationship between the SIA and AWT anomalies fitted to the data from the 1982–91 subperiod (to the left of the bold vertical line).

**Table 1.** Lagged Correlations of the Winter (December–March) Anomalies of Total Sea Ice Area (SIA) in the Nordic Seas ($r_{E+W}$) and in Their Eastern ($r_E$) and Western ($r_W$) Parts With Other Seasonal Indices of Regional Climate Variability[a]

| Variable | Acronym | Lag[b] | $r_{E+W}$ | $r_E$ | $r_W$ |
|---|---|---|---|---|---|
| Atlantic water temperature[c] | AWT | −6 | **−0.86** | **−0.80** | **−0.65** |
| Sea surface temperature[d] | SST | −9 | **−0.86** | **−0.81** | **−0.63** |
| Sea surface temperature[e] | SST | −9 | **−0.74** | −0.51 | **−0.79** |
| Sea surface temperature[f] | SST | −9 | **−0.75** | −0.56 | **−0.75** |
| 'On Ice Wind' index[g] | OIW | −11 | **−0.67** | **−0.74** | −0.34 |
| North Atlantic Oscillation | NAO | −11 | **−0.55** | −0.30 | **−0.71** |

[a]Correlations are for SIA in winters 1982–83 to 2005–06. For $r_{E+W}$, $r_E$, and $r_W$, SIA is defined as sea ice concentration (SIC) integrated over the full domain of Figure 1, and east and west of 15°E, respectively. All indices are based on detrended anomalies of 4-month mean variables. Correlations significant at the 95% (99%) confidence level are bold (and underlined).
[b]In months; negative for the SIA anomalies lagging the other indices.
[c]In the Barents Sea Opening area (BSO box in Figure 1).
[d]Near the Barents Sea ice edge at the cross in Figure 4a.
[e]In the Greenland Sea marginal ice zone (MIZ) at the cross in Figure 4b.
[f]Averaged over the BSO area.
[g]Sea level pressure difference between the southern tips of Novaya Zemlya and Spitsbergen (crosses in Figure 1).

the SIC anomalies integrated east and west of 15°E, respectively. Based on linear correlations ($r$) between the AWT anomalies and time-lagged SIA indices, key postsummer seasons are identified. The local SIC anomalies in these seasons are regressed onto the AWT index and indices of local presummer SST anomalies at key locations. These locations are selected on the basis of the highest correlation between the presummer SST anomalies and the postsummer SIA indices. The statistical significance of all correlations is assessed based on a two-tailed $t$-test carried out with an effective number of degrees of freedom [*Davis*, 1976].

[7] A seasonal NAO index is obtained by 4-month averaging and detrending of the monthly NAO index based on the sea level pressure (SLP) difference between Ponta Delgada, Azores and Stykkisholmur/Reykjavik, Iceland (http://www.cgd.ucar.edu/cas/jhurrell/). Links to wind variability over the Barents Sea are investigated using the On Ice Wind (OIW) index introduced by *Schlichtholz and Houssais* [2011] as the difference in the detrended anomalies of the 4-month mean SLP between the southern tips of Novaya Zemlya and Spitsbergen (Figure 1, crosses). Positive (negative) values of the OIW index correspond to geostrophic wind anomalies across the Barents Sea MIZ directed inward (outward) the ice pack. The SLP data are from the NCEP/NCAR reanalysis [*Kalnay et al.*, 1996]. The OIW index is used as the Barents Sea SIA anomalies in the period under study are more tightly linked to this index than to the index characterizing strength of westerlies into the Barents Sea, introduced by *Bengtsson et al.* [2004] as SLP difference between Spitsbergen and northernmost Norwegian coast.

## 3. Link of Sea Ice Anomalies to AWT Variability

[8] There is a strong link of the summer AWT anomalies in the BSO area to the time lagged SIA anomalies in the Nordic Seas (Figure 3a, circles). The link is significant (see the filled symbols) for the SIA anomalies in presummer seasons, from late winter to early summer (lags −5 to −1 months),

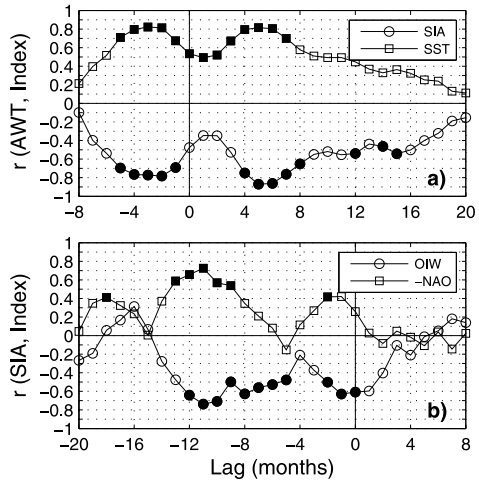


**Figure 3.** Time lagged correlations of (a) the summer index of AWT variability in the BSO area in the 1982–2005 period (Figure 2, circles) with the total SIA (circles) and average SST (squares) anomalies in the Nordic Seas and (b) the winter (December–March) SIA anomalies in the eastern and western parts of the Nordic Seas with the OIW (circles) and NAO (squares) indices, respectively. In Figure 3a, negative (positive) lags correspond to the SST and SIA anomalies leading (lagging) the AWT index. In Figure 3b, negative (positive) lags correspond to the OIW and NAO indices leading (lagging) the SIA anomalies and the sign of $r$ with the NAO index is reversed. In Figures 3a and 3b, filled symbols denote correlations statistically significant at the 95% confidence level.

and also for the SIA anomalies in postsummer seasons, from late autumn to early spring (lags +4 to +8 months). In both cases the correlation is negative, i.e., sea ice retreat (advance) corresponds to warm (cold) AWT anomalies. The correlation is quite high in the presummer seasons when it reaches a maximum ($r = -0.78$) in late spring (lag −2 months) and is even higher in the postsummer seasons when it reaches a peak value of −0.87 at lag +5 months, i.e., in early winter (November–February).

[9] The link of the presummer SIA anomalies to the summer AWT variability reflects anomalous presummer air-sea interactions which strongly affect both the sea ice extent and ocean temperature anomalies in the open water of the Nordic Seas [*Schlichtholz and Houssais*, 2011]. Indeed, the correlation of the time lagged average SST anomalies in these seas with the summer AWT index shows a high presummer maximum ($r = 0.82$) in spring, i.e., at lag −3 months (Figure 3a, squares). This maximum is followed by a significant late summer (lag +1 month) minimum correlation ($r = 0.49$) which suggests that oceanic heat anomalies generated in the presummer seasons partly survive on the surface of the open water through summer. Their survival is however stronger in subsurface layers, as indicated by a considerable increase in the correlation between the postsummer SST anomalies and the summer AWT index (Figure 3a, squares). The increase starts in autumn (lag +3 months) and ends in early winter ($r = 0.81$) and so must mainly result from the surface reemergence of oceanic heat anomalies through entrainment into a deepening mixed layer on the open water side of the ice edge. This process should ultimately lead to the appearance of significant AWT-associated SIC anomalies all along the Nordic Seas MIZ (see the dark shading in Figure 1).

## 4. Link to SST Variability

[10] The scenario in which the postsummer ice cover variability in the Nordic Seas is controlled by the surface reemergence of oceanic heat anomalies is further supported by the patterns of spring (March–June) SST anomalies associated with the following winter (December–March) indices of SIA variability in the eastern and western MIZs (Figures 4a and 4b, respectively). In both patterns, broad areas of significant SST anomalies appear (see the dark shading) and the anomalies locally exceed −0.5°C. In the pattern associated with the eastern SIA index, the largest SST anomalies occur at the ice edge in the western Barents Sea. The highest correlation ($r = -0.81$) is found for the SST anomalies on the open water side of the ice edge in the Hopen Trench area, at the cross in Figure 4a. In the pattern associated with the western SIA index, the largest SST anomalies occur in the Greenland Sea MIZ where the highest correlation (−0.79) is found for the SST anomalies at the cross in Figure 4b.

[11] Significant winter SIC anomalies associated with the previous spring index of SST variability in the Barents Sea (normalized SST anomalies at the cross in Figure 4a) extend over almost the entire Barents Sea MIZ, but reach a maximum (about −20%) off Novaya Zemlya (Figure 4c). This indicates that the presummer oceanic heat anomalies are advected from the western Barents Sea mainly eastward. However, some westward advection may also occur which would be consistent with a strong link of the summer AWT anomalies in the BSO area to both the following winter SIA anomalies in the Barents Sea (Table 1) and the previous spring SST anomalies in the Barents Sea open water [*Schlichtholz and Houssais*, 2011]. The westward export of oceanic heat anomalies via the Hopen Trench recirculation (HTR in Figure 1) may explain why the winter total SIA anomalies in the Nordic Seas correlate higher with the previous summer AWT anomalies in the BSO area and the previous spring SST anomalies in the Hopen Trench area ($r = -0.86$ for both the AWT and SST anomalies) than the corresponding SIA anomalies in the Barents Sea alone do (Table 1).

[12] Significant winter SIC anomalies associated with the previous spring index of SST variability in the Greenland Sea MIZ (normalized SST anomalies at the cross in Figure 4b) appear in the whole western MIZ, but are the largest (above −15%) in bands extending from the southwestern Greenland Sea to the south and east (Figure 4d). These bands could result from the surface reemergence of oceanic heat anomalies generated in the presummer Greenland Sea MIZ and then advected southward and eastward by the East Greenland and Jan Mayen currents, respectively. The postsummer SIC anomalies in the northwestern Greenland Sea should mainly result from the surface reemergence of oceanic heat anomalies advected from the east by the Return Atlantic Current (RAC in Figure 1). This is suggested by significant spring SST anomalies

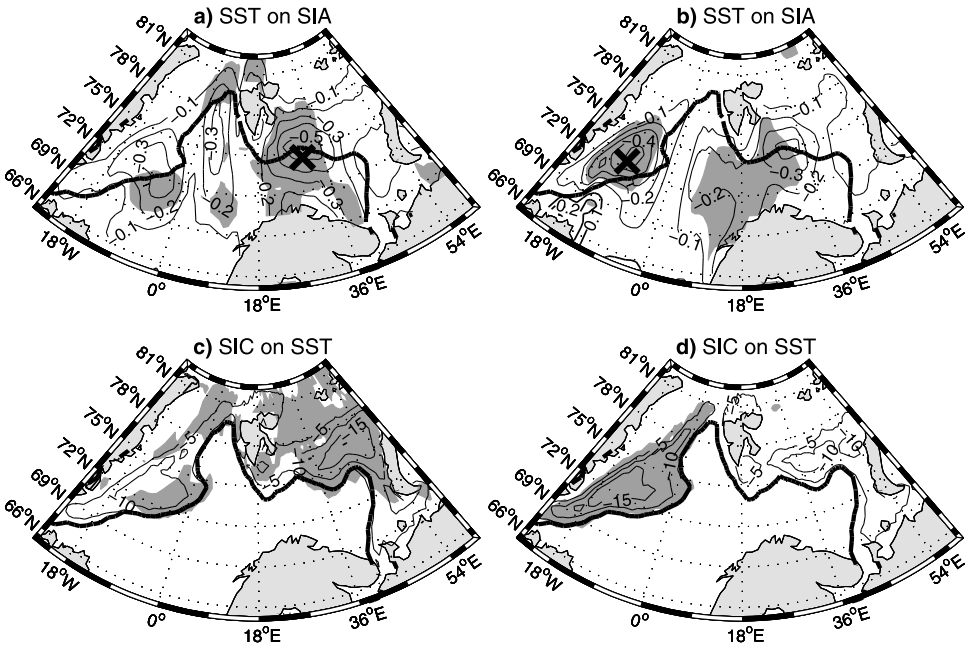


**Figure 4.** Spring (March–June) SST anomalies in the Nordic Seas area regressed onto the following winter indices of SIA variability in the (a) eastern and (b) western parts of the Nordic Seas and winter SIC anomalies regressed onto the previous spring indices of SST variability in the (c) Barents and (d) Greenland seas in the 1982–2005 period. In Figures 4a–4d, thin (thick) contours correspond to negative (positive) anomalies, the zero contour is omitted, dark shading denotes anomalies statistically significant at the 95% confidence level, and the very thick line shows the climatological mean position of the ice edge (5% SIC contour) in spring (Figures 4a and 4b) or winter (Figures 4c and 4d)). The contour interval is 0.1°C per unit SIA index in Figures 4a and 4b and 5% per unit SST index in Figures 4c and 4d. In Figures 4a and 4b, the crosses indicate the locations of maximum correlation between the spring SST anomalies and the following winter SIA anomalies in the eastern and western parts of the Nordic Seas, respectively. The normalized (divided by their standard deviation) SST anomalies at these locations are used as the indices for construction of the SST-associated SIC anomalies in Figures 4c and 4d, respectively.

associated with the following winter index of the western SIA anomalies which appear in ($r = -0.75$) and around the BSO area (Figure 4b).

## 5. Link to Atmospheric Forcing

[13] Oceanic heat anomalies which control the postsummer sea ice variability in the Nordic Seas are mainly generated by presummer atmospheric forcing. In the Barents Sea, anomalous late winter (January–April) on ice winds lead to strong turbulent surface heat flux anomalies in the open water [*Schlichtholz and Houssais*, 2011]. The SST response to this forcing is delayed due to a high ocean heat capacity. The response is extreme in spring when the pattern of SST anomalies associated with the late winter OIW index (not shown) resembles the pattern of spring SST anomalies associated with the following winter index of eastern SIA variability (Figure 4a). Consequently, the winter SIA anomalies in the Barents Sea are strongly linked to the previous late winter on ice wind anomalies. Indeed, their peak correlation with the OIW index ($r = -0.74$) occurs at lag −11 months (Figure 3b, circles).

[14] The winter SIA anomalies on the western side of the Nordic Seas are strongly linked to the previous late winter NAO forcing, as shown by their peak correlation with the NAO index ($r = -0.71$) at lag −11 months (see Figure 3b, squares, and notice the reversed sign of $r$). This link should mainly result from the reemergence of SST anomalies as the pattern of spring SST anomalies associated with the previous late winter NAO index (not shown) is similar to the pattern of spring SST anomalies associated with the following winter index of western SIA variability (Figure 4b).

## 6. Conclusions

[15] The lead-lag correlation analysis applied to observational timeseries of seasonal mean variables has revealed that recent (1982–2005) variability of summer temperature in the Atlantic water core (AWT anomalies) downstream of the Norwegian Atlantic Current (BSO area) explains ~75% of the variance of the Nordic Seas ice cover (SIA anomalies) in the following winter and that this link to a large extent reflects forcing of sea ice variability by postsummer reemergence of previous spring SST anomalies (Figures 3a and 4). These spring anomalies are generated by late winter atmospheric forcing. The late winter NAO index explains ~50% of the following winter SIA variance in the Greenland Sea while ~50% of the winter SIA variance in the Barents Sea is explained by the previous late winter OIW index characterizing strength of anomalous winds across the Barents Sea ice edge (Table 1 and Figure 3b).

[16] The links found here do not only improve our understanding of the interannual climate variability in the Nordic Seas area, but can also be used to perform effective seasonal forecasts of regional sea ice cover. A simple example is shown in Figure 2 where the observed early

winter SIA anomalies in the Nordic Seas in the 1992–2005 (calendar years of the beginning of winter) period (see the squares to the right of the bold vertical line and notice the reversed sign of the SIA anomalies) are compared to their prediction (stars) from the previous summer AWT index (circles to the right of the bold vertical line). The prediction is based on a linear model of the statistical relationship between the two variables 'trained' on the data from the 1982–91 period (circles and squares to the left of the bold vertical line). The high correlation skill score (0.85) and proportion of explained variance (71%) of this prediction are indeed promising.

[17] A question is whether the links reported here are robust. The period under study falls on the years of Arctic amplification of global warming [e.g., *Johannessen et al.*, 2004] and the general intensification of the thermohaline conveyor in the North Atlantic [e.g., *Zhang et al.*, 2004]. However, even in this period of strong Atlantic water inflow to the Nordic Seas, the interannual oceanic heat variability downstream of the Norwegian Atlantic Current depended more on the regional air-sea interactions than on the transport of heat anomalies from the south [*Schlichtholz and Houssais*, 2011]. Strong variability of these interactions on interannual to decadal timescales might have been induced by feedbacks with the recent Arctic sea ice reduction trend [*Wang et al.*, 2005]. Optimal sea ice predictors and their skills may vary over time, but it is unlikely that strong oceanic influence on sea ice cover in the Nordic Seas was limited to the recent decades. For instance, a numerical simulation of the early 20th-century warming in the Arctic shows that this warming was maintained by self-sustaining regional climate feedbacks triggered by a wind-driven increase of oceanic heat flux to the Barents Sea and subsequent sea ice retreat [*Bengtsson et al.*, 2004].

[18] The links studied here may change in the future climate regime with accelerated Arctic sea ice shrinking. This acceleration might have already started as indicated by an abrupt decline of summertime Arctic sea ice in 2007 [*Comiso et al.*, 2008]. However, the strong link of winter sea ice anomalies in the Nordic Seas to oceanic heat variability seems to hold up till present. Indeed, inspection of *Reynolds et al.*'s [2002] dataset updated to 2010 indicates that the Nordic Seas SIA anomalies in the last four winters were not exceptional and that the maximum correlations of the winter SIA anomalies in the Barents and Greenland seas with the preceding spring SST anomalies estimated for the entire 1982–2010 period (not shown) are practically the same as for the 1982–2006 period (Table 1). This is consistent with a climate model study which shows that while predictability of summer Arctic sea ice cover should decrease in the regime of accelerating sea ice decline, predictability of winter cover may not [*Holland et al.*, 2010].

[19] **Acknowledgments.** The AWT index is based on hydrographic data from the International Council for the Exploration of the Sea (http://www.ices.dk/) and the National Oceanographic Data Center of NOAA, US (http://www.nodc.noaa.gov/). The SST, SIC and SLP data were provided by the NOAA-CIRES ESRL/PSD Climate Diagnostics branch (http://www.cdc.noaa.gov/) and the NAO index by the Climate and Global Dynamics division of NCAR (http://www.cgd.ucar.edu/cas/jhurrell/).

[20] Eric Rignot thanks two anonymous reviewers.

## References

Bengtsson, L., V. A. Semenov, and O. M. Johannessen (2004), The early twentieth-century warming in the Arctic—A possible mechanism, *J. Clim.*, *17*, 4045–4057.

Comiso, J. C., C. L. Parkinson, R. Gersten, and L. Stock (2008), Accelerated decline in the Arctic sea ice cover, *Geophys. Res. Lett.*, *35*, L01703, doi:10.1029/2007GL031972.

Davis, R. E. (1976), Predictability of sea surface temperature and sea level pressure anomalies over the North Pacific Ocean, *J. Phys. Oceanogr.*, *6*, 249–266.

Drobot, S., J. Stroeve, J. Maslanik, W. Emery, C. Fowler, and J. Kay (2008), Evolution of the 2007–2008 Arctic sea ice cover and prospects for a new record in 2008, *Geophys. Res. Lett.*, *35*, L19501, doi:10.1029/2008GL035316.

Holland, M. M., C. M. Bitz, and B. Tremblay (2006), Future abrupt reductions in the summer Arctic sea ice, *Geophys. Res. Lett.*, *33*, L23503, doi:10.1029/2006GL028024.

Holland, M. M., D. A. Bailey, and S. Vavrusand (2010), Inherent sea ice predictability in the rapidly changing Arctic environment of the Community Climate System Model, version 3, *Clim. Dyn.*, doi:10.1007/s00382-010-0792-4.

Hurrell, J. W., Y. Kushnir, G. Ottersen, and M. Visbeck (2003), An overview of the North Atlantic Oscillation, in *The North Atlantic Oscillation: Climatic Significance and Environmental Impact*, *Geophys. Monogr. Ser.*, vol. 134, edited by J. W. Hurrell et al., pp. 1–35, AGU, Washington, D. C.

Johannessen, O. M., et al. (2004), Arctic climate change: Observed and modelled temperature and sea-ice variability, *Tellus, Ser. A*, *56*, 328–341.

Kalnay, E., et al. (1996), The NCEP/NCAR 40-yr reanalysis project, *Bull. Am. Meteorol. Soc.*, *77*, 437–471.

Lindsay, R. W., J. Zhang, A. J. Schweiger, and M. A. Steele (2008), Seasonal predictions of ice extent in the Arctic Ocean, *J. Geophys. Res.*, *113*, C02023, doi:10.1029/2007JC004259.

Petoukhov, V., and V. A. Semenov (2010), A link between reduced Barents-Kara sea ice and cold winter extremes over northern continents, *J. Geophys. Res.*, *115*, D21111, doi:10.1029/2009JD013568.

Reynolds, R. W., N. A. Rayner, T. M. Smith, D. C. Stokes, and W. Wang (2002), An improved in situ and satellite SST analysis for climate, *J. Clim.*, *15*, 1609–1625.

Schlichtholz, P., and M.-N. Houssais (2011), Forcing of oceanic heat anomalies by air-sea interactions in the Nordic Seas area, *J. Geophys. Res.*, *116*, C01006, doi:10.1029/2009JC005944.

Serreze, M. C., M. M. Holland, and J. Stroeve (2007), Perspectives on the Arctic's shrinking sea-ice cover, *Science*, *315*, 1533–1536.

Sorteberg, A., and B. Kvingedal (2006), Atmospheric forcing on the Barents Sea winter ice extent, *J. Clim.*, *19*, 4772–4784.

Vengas, S. A., and L. A. Mysak (2000), Is there a dominant timescale of natural climate variability in the Arctic?, *J. Clim.*, *13*, 3412–3434.

Vinje, T. (2001), Anomalies and trends of sea-ice extent and atmospheric circulation in the Nordic Seas during the period 1864–1998, *J. Clim.*, *14*, 255–267.

Wang, J., M. Ikeda, S. Zhang, and R. Gerdes (2005), Linking the Northern Hemisphere sea-ice reduction trend and the quasi-decadal arctic sea-ice oscillation, *Clim. Dyn.*, *24*, 115–130.

Wu, B., J. Wang, and J. Walsh (2004), Possible feedback of winter sea ice in the Greenland and Barents Seas on the local atmosphere, *Mon. Weather Rev.*, *132*, 1868–1876.

Zhang, J., M. Steele, D. A. Rothrock, and R. W. Lindsay (2004), Increasing exchanges at Greenland-Scotland Ridge and their links with the North Atlantic Oscillation and Arctic sea ice, *Geophys. Res. Lett.*, *31*, L09307, doi:10.1029/2003GL019304.

Zhang, J., M. Steele, R. Lindsay, A. Schweiger, and J. Morison (2008), Ensemble 1-Year predictions of Arctic sea ice for the spring and summer of 2008, *Geophys. Res. Lett.*, *35*, L08502, doi:10.1029/2008GL033244.

P. Schlichtholz, Institute of Oceanology, Polish Academy of Sciences, Powstancow Warszawy 55, 81-712 Sopot, Poland. (schlicht@iopan.gda.pl)